Periodica Polytechnica
Civil Engineering

Colour of Stone Slabs under Different Standard Illuminations

61(1), pp. 66–74, 2017
DOI: 10.3311/PPci.9038

Ákos Antal[1*], Péter Görög[2], Ádám László Veres[1], Petra Balla[1]
Ákos Török[2]

RESEARCH ARTICLE

Received 20-01-2016; accepted 08-03-2016

Abstract

Spectral measurements have been carried out on polished stone slabs to show the accuracy of theoretical colorimetric calculations on perceptual differences of color appearance under various standard illuminations. Effects of the different spectral characteristics of the light source on colorization of the samples have been also studied to analyze the changes of color sensation on the samples in connection with the changes on the type of the illuminating source. Solar light (Standard Illuminant D65), basic incandescent source (Standard Illuminant A) and a basic fluorescent source (Standard Illuminant F11) have been tested on Tardos red limestone, Siklós green limestone, Carrara white and gray marbles and diorite samples. Colorizing effects of the examined illuminations are compared to Standard Illuminant E – the theoretically perfect white source.

Keywords

colour appearance, colour difference, limestone, marble, diorite

[1]Department of Mechatronics, Optics and Engineering Informatics
Budapest University of Technology and Economics
H-1521 Budapest, P.O.B. 91, Hungary
[2]Department of Engineering Geology and Geotechnics
Budapest University of Technology and Economics
H-1521 Budapest, P.O.B. 91, Hungary
*Corresponding author, e-mail: antalakos@antalakos.hu

1 Introduction

Stone slabs are frequently used for cladding outside and inside buildings. From architectural point of view the most important parameters for design of natural stone cladding are the optical properties of stone slabs. The appearance and optical properties can be controlled by naked eye according to Eurocode EN1469. More recently, Zamora-Mestre et al. [1] introduced a new method for the optical quality control, which measures the optical appearance of the slabs by image processing software. It helps to avoid the visual anomalies of the stone slabs, but the appearance of the cladding depends on the actual light conditions. The external cladding looks different under sunshine and in cloudy weather conditions. When the cladding is placed inside a building the artificial lighting of the interior should be synchronized with the optical properties of the stone slabs. The present paper describes the optical appearance of different stone slabs under different lighting conditions. The main goal of this study is to give an advice how to select a stone slab based on colour difference or chroma when different types and different intensity of illuminations are applied.

The spectroscopy can be used for studying the variations in colour of stone slabs under different artificial lights. It is also a useful tool to measure the grade of weathering as it is described for granitic rocks by Nagano and Nakashima [2].

Different types of limestones, marble and diorite are commonly used for cladding both for indoor and outdoor. Natural and aesthetic appearance and outstanding durability of these stones make them perfect to create durable and spectacular coating even on large surface areas.

However, appearance is strongly related to the applied illumination. From sunlight to the wide range of fluorescent and incandescent sources, the spectral power distribution of the incoming light varies between wide boarders – and consequently the colour sensation provided by the cladding material can vary heavily under different illuminations.

Furthermore, analysing these effects is not always easy and straightforward. Only complex theoretical colorimetric calculations can be applied during the design phase of an object, real “on-site” measurements are usually problematic before the

implementation. Regarding to the heavily theoretical nature of these calculations, it is reasonable to show the accuracy of them. Therefore simulated environments were created for the samples, to describe the theoretically considered conditions in real life and compare the two different sets of data – theoretical versus direct, "life-like" measurements.

It is also reasonable to compare the stability of the chromatic characteristic of the samples under different illuminations. Thus, the differences in colorization and chroma against the theoretically perfect white illumination (Illuminant E) were compared. These calculations can show which sample has the most illuminant independent chromatic characteristic, i.e. which stone slab visual appearance is the most similar under differently illuminated environments.

2 Methodology

2.1 Measurement setup

Colorimetric calculations were made based on the spectral intensity distribution of the light reflected from the measured surfaces., Several types of colour coordinates were calculated – directly from the XYZ coordinates, or – the ones represented in the corresponding colour spaces – e.g. in CIE L*a*b* [3].

Spectral reflectance measurements were made on all of the samples to get their "relative" – illumination independent – reflection spectra. This raw data gives the possibility to calculate the appearance of the samples under different standard illuminations in a theoretical way. A Konica Minolta CM-2500d handheld spectrometer was used to collect the absolute spectral data. The measurements were carried out with a 2° wide aperture, in 45° measurement configuration, and the data was processed with the scattering components included.

The "absolute" spectral reflectance of the samples under different standard illuminations [4] was also measured. The aim was to record the spectral data directly reflected from the surfaces – to simulate the behaviour of the samples during a standard visual inspection, and to make a comparison between theoretically calculated values and the results of the corresponding real measurements. A Gretag Machbet Colour Box was used to produce D65 (similar to solar light), Illuminant A (typical incandescent source) and TL84 (typical fluorescent source) [5] spectra (Fig. 1). The reference spectral data for both illuminations were recorded on a $BaSO_4$ covered white etalon.

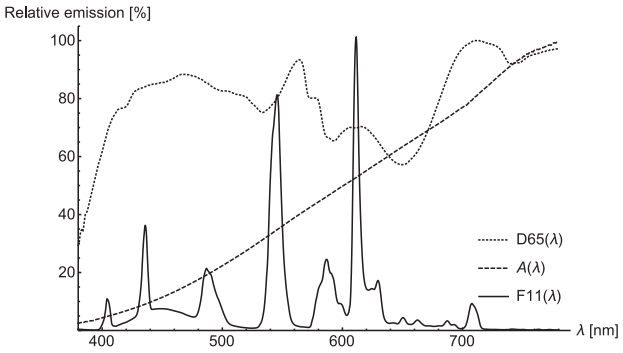

Fig. 1 Measured spectra of the applied sources

These illuminations represent a good general approximation for the usual outdoor light, and the two commonly used indoor light source families [6]. Standardized forms of their spectral characteristics are also available – these data were used for the theoretical calculation (Fig. 2).

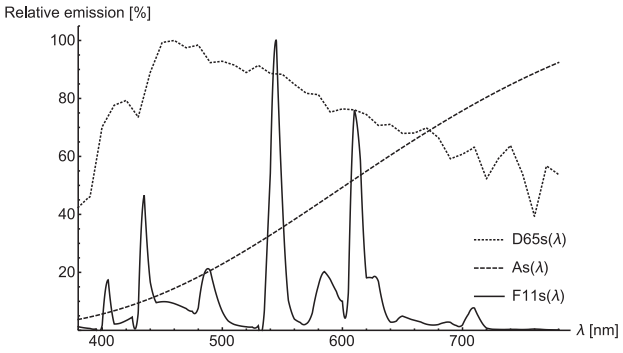

Fig. 2 Standardized spectra of the applied illuminations

A Konica Minolta CS-1000 spectroradiometer camera was used to record the reflected spectral data. This device uses a calibrated standard photography objective lens to collect the incoming light from the measurement area (1° wide) and therefore makes it possible to adjust the exact position and relative size of it.

The inspected samples were placed inside the Colour box on a rotatable holder. The illumination came from the topside of the box, and the rotatable holder was set to ensure 45° angle of incidence. The spectroradiometer camera was placed 120 cm away from the centre of the sample, and the height of the instrument was set to be on the same level with the measured specimen.

The target-instrument distance – consequently the measurement area of the CS-1000 instrument – was selected to cover a reasonably large region on the measured sample surface with the measurement area (Fig. 3).

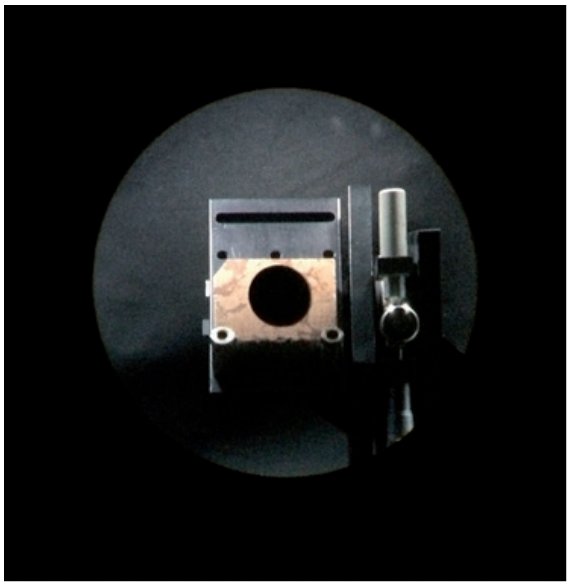

Fig. 3 Measurement area

Ten measurements were carried out under both illuminations on all of the samples – with constant repositioning of the measurement area. The collected spectral data were used to calculate x and y, and L* a* b* values for further analysis.

2.2 Calibration of the instruments

Two different types of spectral measurements were carried out: one for the pure reflectance spectra of the samples; and one for the "life-like" absolute reflectance, which included the characteristics of the illuminating source as well. These two methods required different calibration processes.

The illumination independent reflection spectra measurement is a relative measurement, which means the measured spectral data is given from nanometer to nanometer as a percentage of the instrument's built-in illuminating source's spectral characteristic. To record the pure spectra of the source as a reference, a white calibration is required from time to time. To calibrate the instrument, a nearly-perfectly reflective white reference surface is needed with very flat spectral characteristic through the whole measurement range. This is usually a small BaSO4 covered disk, which is a standard accessory of the instrument.

Handheld spectrophotometers like the Konica Minolta CM-2500d are usually also able to do a dark calibration, which is for eliminating the dark noise of their detector. In our case, both white and dark calibrations were done before the measurements – to get the best possible accuracy.

The absolute reflectance measurement however does not require such calibrations. Since this process is a direct measurement the light reflected directly from the measured surface contains all of the necessary information – no further processing required.

The accuracy of the instrument is guarantied with a calibration to a standard source. With the Konica Minolta CS-1000, two different type of calibration is possible – wavelength calibration, and level calibration. The former is to adjust the measurement data (taken with the use of the standard source) alongside the wavelength axis to match with the data preloaded (practically based on the documentation of the standard source). The same stands for the level calibration, but in this case the intensity values are matched to calibrate the data on the vertical axis. We used the CS-1000 in absolute mode with factory calibration, with which the vertical axis represented spectral radiance in [$W/m^2sr\,nm$].

However, the absolute radiometric values were available, we did not use such data for any kind of calculations – just to represent the measured spectra. Since color data is independent from the intensity of the illumination it is indifferent from the colorimetric point of view in our case. The software calculates X, Y and Z coordinates directly, and we used these data instead of calculating these values from the spectral data manually. This method gives a more life-like comparison between fully calculated and purely measured data.

2.3 Description of the applied colour systems

The quantitative representation of colour data is always a challenge – due to the subjective nature of human colour vision. However, there are few perceptually evident fundaments, which help to create generally usable systems to mathematically characterize the colour sensations. Some of these systems are standardized by the International Commission on Illumination (CIE), and commonly used in colour science.

Most of the commonly used colour spaces are based on the CIE 1969 trichromatic system also known as the refined CIE XYZ space for 10° observer – which is an adjusted version of the first standardized approximation of colour perception. This system is based on the trichromatic behaviour of colour vision, and formed with a series of colour matching experiments, where the participants had to adjust the intensity of three perceptually independent monochromatic light sources until the sense of the mixture of the three primary colours are match with a dedicated monochromatic light.

With the repentance of this match – from one monochromatic stimulus to another – through the complete visible spectrum, three sets of colour matching functions [7] where presented – $\overline{r}(\lambda)$, $\overline{g}(\lambda)$ and $\overline{b}(\lambda)$ (Fig. 4). Since $\overline{r}(\lambda)$, $\overline{g}(\lambda)$ and $\overline{b}(\lambda)$ functions have negative values at some section of the visible spectra, it is reasonable to transform them to positive values only. This transformation provides $\overline{x}(\lambda)$, $\overline{y}(\lambda)$ and $\overline{z}(\lambda)$ functions (Fig. 5).

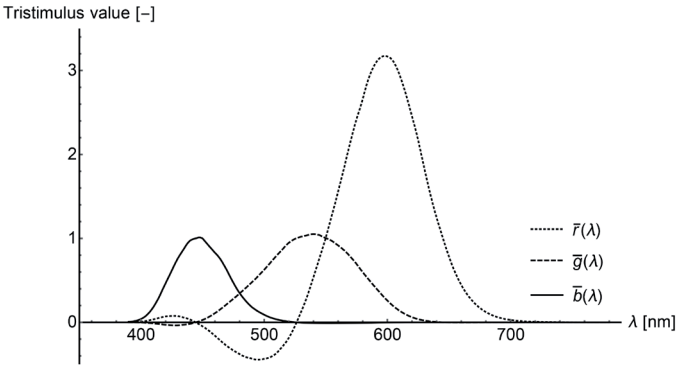

Fig. 4 $\overline{r}(\lambda)$, $\overline{g}(\lambda)$ and $\overline{b}(\lambda)$ CMFs

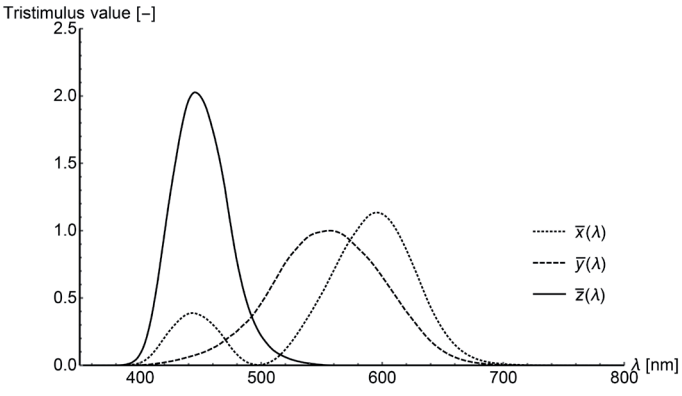

Fig. 5 $\overline{x}(\lambda)$, $\overline{y}(\lambda)$ and $\overline{z}(\lambda)$ CMFs

As it is described before under subchapter 2.3, X, Y and Z refined tristimulus values are calculated as the integral of the corresponding colour matching functions – $\overline{x}(\lambda)$, $\overline{y}(\lambda)$ and $\overline{z}(\lambda)$ – multiplied by the spectral intensity distribution of the light stimulus to inspect.

However, X, Y and Z values represents a 3D space and describes a dedicated stimulus completely, it is not easy to imagine, or show the colour data directly with them. X, Y and Z are absolute values, containing not only colour related, but intensity information as well – which we are usually not interested in. To get a better option to represent colours, it is reasonable to give a normalized version of the tristimulus values – the x, y and z chromaticity coordinates.

$$x = \frac{X}{X+Y+Z} \tag{1}$$

$$x = \frac{Y}{X+Y+Z} \tag{2}$$

$$z = \frac{Z}{X+Y+Z} \tag{3}$$

The x and y coordinates forms the chromaticity diagram of the CIE 1969 trichromatic system, which is unequivocal enough to represent colour data (Fig. 6).

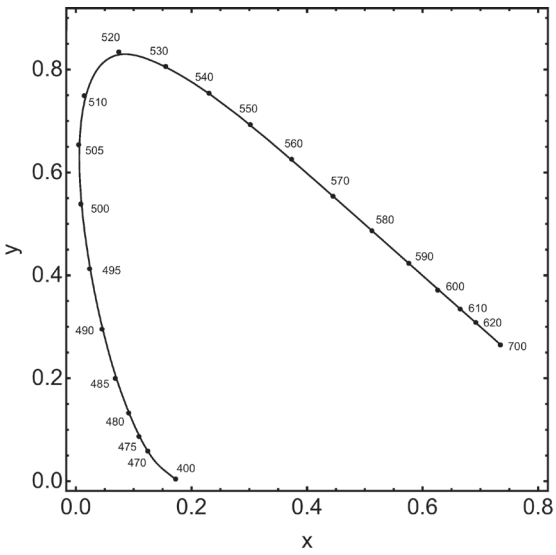

Fig. 6 xy chromaticity diagram

Since the XYZ space is a very basic approximation of the colour vision – uses only the trichromatic phenomenon, as a hooking point to the neural basis of vision – there are a few derived colour systems developed during the last century. One of these refined colour spaces is the CIE L*a*b* space. CIE L*a*b* is based on the XYZ space and can be created with a linear transformation of it – as it is shown before under subchapter 2.3.

CIE L*a*b* can be adjusted to represent colours under different illuminations more accurately than XYZ. Furthermore, the white point of the space for a dedicated illumination always takes place at the origin.

L*a*b* is a more advanced model from the psychophysical point of view as well. Beside the trichromat nature of human colour vision, L*a*b* represents a deeper level of neurology of the human visual system – the opponent channels. L* is refers to lightness, a* represents red colour stimuli towards its positive direction and green colour stimuli towards the negative direction, the positive direction of the b* coordinate points towards yellow stimuli, and the negative side points to the direction of blue stimuli (Fig. 7).

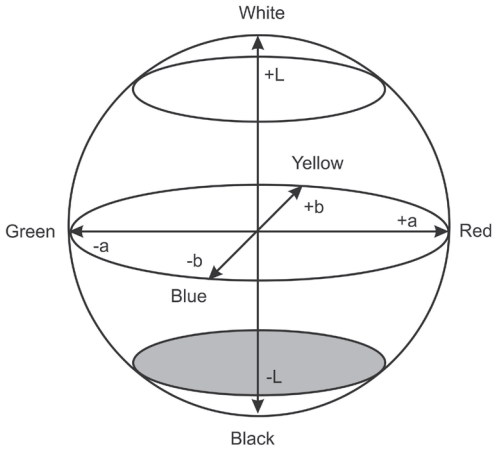

Fig. 7 L*a*b* color space

There is another important difference between XYZ and L*a*b*. Just like most of the colour spaces, XYZ and L*a*b* are represent visible colours as a Euclidian space – however, an ideal colour space would be a Riemann-like one. This phenomenon entails that both XYZ and L*a*b* are nonlinear spaces from the practical point of view [8].

The main aim of the transformation to L*a*b* is to decreases the nonlinearities of the colour space compared to XZY, therefore distances between two different point of the L*a*b* space represents real perceptual colour differences much better. Consequently, it is reasonable to calculate ΔE colour differences [9] in L*a*b* spaces – to predict, analyse or simply show quantitative differences between different colour stimuli.

2.4 Calculating colour data

The measured relative spectral data contains only the reflectance characteristic of the sample. To get exact colorimetric data under a specified illumination a spectral characteristic of the light source used should be taken into consideration. To do so, the spectral power distributions (SPD) of the source and the sample have to be combined in the following way

$$\Phi_\lambda(\lambda) = R_s(\lambda) E_{ls}(\lambda) \tag{4}$$

Where $E_{ls}(\lambda)$ is the SPD of the selected standard illumination and $R_s(\lambda)$ is the SPD of the investigated sample.

Once the calculated absolute reflectance spectra is available, X, Y and Z tristimulus values for the CIE 1969 10° standard colorimetric observer can be calculated with the following steps

$$\begin{bmatrix} \bar{x}(\lambda) \\ \bar{y}(\lambda) \\ \bar{z}(\lambda) \end{bmatrix} = \begin{bmatrix} 0.341080 & 0.189145 & 0.387529 \\ 0.139058 & 0.837460 & 0.073160 \\ 0 & 0.039553 & 0.026200 \end{bmatrix} \begin{bmatrix} \bar{r}(\lambda) \\ \bar{g}(\lambda) \\ \bar{b}(\lambda) \end{bmatrix} \tag{5}$$

$$X = 683.6 \int_{380nm}^{780nm} \Phi_\lambda(\lambda) \bar{x}(\lambda) d\lambda \tag{6}$$

$$Y = 683.6 \int_{380nm}^{780nm} \Phi_\lambda(\lambda) \bar{y}(\lambda) d\lambda \tag{7}$$

$$Z = 683.6 \int_{380nm}^{780nm} \Phi_\lambda(\lambda) \bar{z}(\lambda) d\lambda \tag{8}$$

Where $\bar{r}(\lambda)$, $\bar{g}(\lambda)$ and $\bar{b}(\lambda)$ are the experimental colour matching functions (CMFs), $\bar{}(\ )$, $\bar{y}(\lambda)$ and $\bar{z}(\lambda)$ are the CMFs of the CIE 1969 10° standard colorimetric observer.

In this way, both the directly measured and a calculated X, Y and Z values are available. To calculate the L*a*b* coordinates, the X_n, Y_n and Z_n coordinates for the specified white object is also needed. To analyse all of the investigated illuminations alongside each other, Illuminant E is the perfect choice to use to get white object data. Illuminant E is the theoretically perfect white source, with even characteristics on all wavelengths; therefore X_n, Y_n and Z_n values are both equals to 1.

$$L^* = 116 f(Y/Y_n) - 16 \tag{9}$$

$$a^* = 200\left[f(X/X_n) - f(Y/Y_n) \right] \tag{10}$$

$$b^* = 200\left[f(Y/Y_n) - f(Z/Z_n) \right] \tag{11}$$

Where

$$\begin{aligned} &f(X/X_n) = (X/X_n)^{1/3} \\ &if \ \ (X/X_n) > (24/116)^3 \end{aligned} \tag{12}$$

$$\begin{aligned} &f(X/X_n) = (841/108)(X/X_n)^{1/3} + 16/116 \\ &if \ \ f(X/X_n) \le (24/116)^3 \end{aligned} \tag{13}$$

$$\begin{aligned} &f(Y/Y_n) = (Y/Y_n)^{1/3} \\ &if \ \ (Y/Y_n) > (24/116)^3 \end{aligned} \tag{14}$$

$$\begin{aligned} &f(Y/Y_n) = (841/108)(Y/Y_n)^{1/3} + 16/116 \\ &if \ \ f(Y/Y_n) \le (24/116)^3 \end{aligned} \tag{15}$$

$$\begin{aligned} &f(Z/Z_n) = (Z/Z_n)^{1/3} \\ &if \ \ (Z/Z_n) > (24/116)^3 \end{aligned} \tag{16}$$

$$\begin{aligned} &f(Z/Z_n) = (841/108)(Z/Z_n)^{1/3} + 16/116 \\ &if \ \ f(Z/Z_n) \le (24/116)^3 \end{aligned} \tag{17}$$

In the L*a*b* space it is possible to calculate chromatic and colorization differences as Euclidian distances between two points – representing two different colour sensations. The equations for ΔE (total colour difference) and ΔC (Chroma difference) are the following.

$$\Delta E^* = \sqrt{(\Delta L^*)^2 + (\Delta a^*)^2 + (\Delta b^*)^2} \tag{18}$$

$$\Delta C^* = C_1^* - C_2^* = \sqrt{(a_1^*)^2 + (b_1^*)^2} - \sqrt{(a_2^*)^2 + (b_2^*)^2} \tag{19}$$

3 Materials

Stone slabs of five different rock types were investigated: Tardos red limestone, Siklós green limestone, a white and a grey marble from Carrara, and grey diorite from Italy. All studied stone slabs were polished, having the same surface finish (Fig. 8).

The Tardos red limestone is a very common dimension stone in the Carpathian Region. This Jurassic limestone has been exploited from the Roman period in Gerecse Mountains, North Hungary having various shades of red colour (Fig. 8, S29, S30, S31).

It was commonly termed as "red marble" of Hungary [10]. The red colour and aesthetics made this stone as one of the favorite dimension stones of Roman period and medieval kings of Hungary [11]. One example is the red "marble" fountain in the Castle of Visegrád which was made from this stone during the reign of King Matthias [11]. It has been also used at other sites such as the cathedral of Nitra [12].

The Siklós "green" limestone is quarried in the Villány Mountains, South Hungary. It represents thick bedded cemented limestones of Middle Triassic Zuhánya Limestone Formation (Fig 8. S 1377). This popular limestone shows great variety in colour, the most common types are the brownish-grey, grey slightly greenish ones. There are irregular mottles in the matrix having slightly lighter colour as a rule, i.e. pale yellow to pinkish mottles also occur. Besides the mottles of centimetre to 45 cm in size, brachiopods are also common [13]. Dolomitization occurs in micritic mottles and also along fissures representing several phases of dolomite formation [14]. The physical properties of the Siklós green limestone were described in [13]. The uniaxial compressive strength is 80 MPa, but after 25 freeze-thaw cycles it is reduced by 37%. Hence, it is no frost resistant, but can be used only for inner cladding.

The Carrara Marble one of the most famous dimension and ornamental stone of the world. In the medieval architecture mainly it was used in Europe in the Italian region, but nowadays it can be found all over the world [15]. Carrara marble is still used in large quantities in modern buildings (in Mekka at mosques, Opera House in Oslo). Rosso et al. [16] investigated the energy-efficiently of white marble used as facing stones on the facade of a new building in New York. The properties of the Carrara marble were described and studied in details. Karaca et al. [17] studied the micro-fabric; the grain properties and the grain boundaries of different types of marbles. Cardani and Meda [18] measured the flextural strength of the Carrara marble, while Leiss and Weiss [19] evaluated the fabric anisotropy and the thermal induced degradation.

In this paper two different types of Carrara marbles were studied a white one (Fig. 8, S56) and a grey one (Fig. 8, S55). The white one is micro-crystalline with fairly homogenous micro-fabric. The grey marble of Carrara was described in detail by means of petrographic methods by Borghi [20].

The diorite is an intermediate plutonic rock, with prevailing minerals of plagioclase and pyroxene. The studied slab represents a dark grey variety, which has the darkest colour compared to the other specimens (Fig. 8, S861).

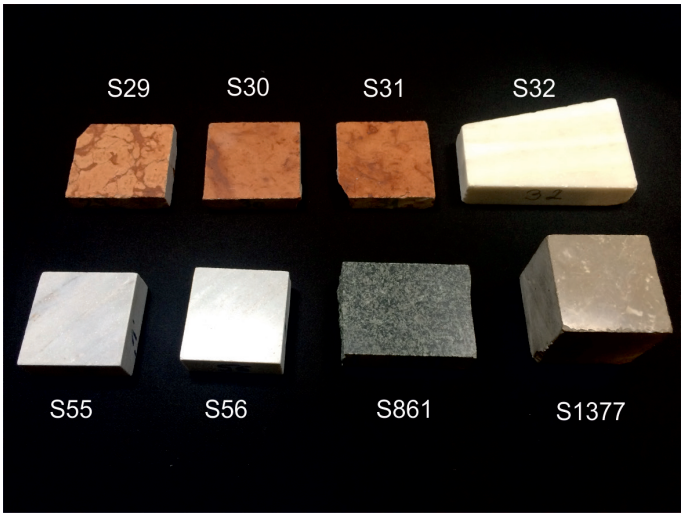

Fig. 8 Investigated stone slabs
(S29-S31: Tardos red limestone; S32: white Carrara marble; S55-S56: grey Carrara marble; S861: diorite; S1377: Siklós greenlimestone)

The samples can be divided into two different groups based on their visual appearance. The measured reflectance spectra of the stones coincide with this grouping.

The spectra of the three red limestones are nearly identical. The greenish grey limestone has a bit different reflection characteristic, but clearly fits between the other three samples (Fig. 9).

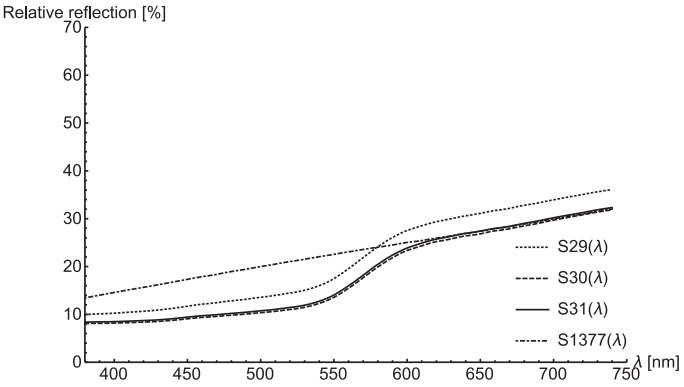

Fig. 9 Relection spectra of red Tardos limestones (S29, S30, S31) and greenish grey Zuhánya limestone (S1377)

The white marble from Carrara has a much higher reflexion value than the grey marble, but the spectra of the grey Carrara marble is more flat. Diorite is much less reflective than the other samples, but its flat characteristic clearly fits into this group (Fig. 10).

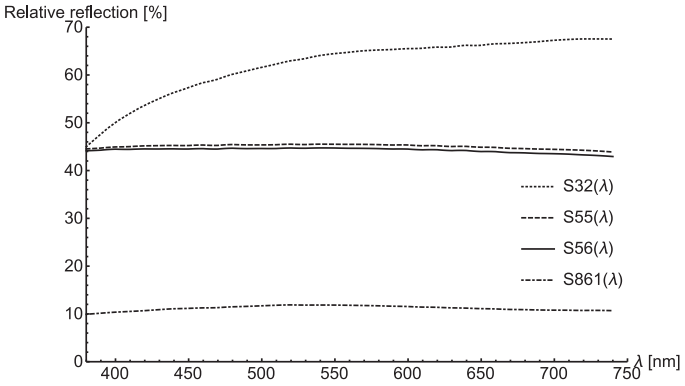

Fig. 10 Relection spectra of white marble (S32), grey Carrara marble (S55), white Carrara marble (S56) and grey diorite (S861)

4 Results

Comparison between the directly measured and calculated x and y chromaticity coordinates shows that the theoretically calculated data is accurate enough even for complex simulations. Fig. 11 and Fig. 12 show the two different dataset alongside each other for samples S29, S30 and S31 in the xy chromaticity diagram. It is clearly visible that the calculated and measured points are perfectly lapping each other for illumination D65, and the points are relatively close for Illuminant A as well. However, for F11 the separation between the measured and calculated data requires some explanations.

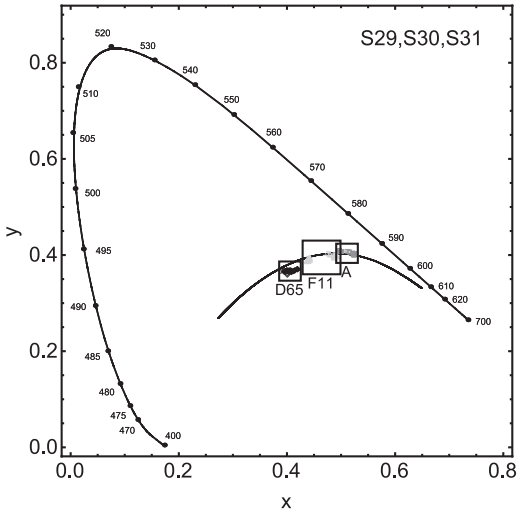

Fig. 11 xy chromaticity data for S29, S30 and S31

If we compare the theoretical spectra of the F11 standard illumination, and the measured data from the same source, the distributions are noticeably different (Fig. 13). The height of the two main peaks of the spectra shows an opposite trend, therefore the total energy distribution of the measured spectra shifts towards the higher wavelength region compared to the theoretical one.

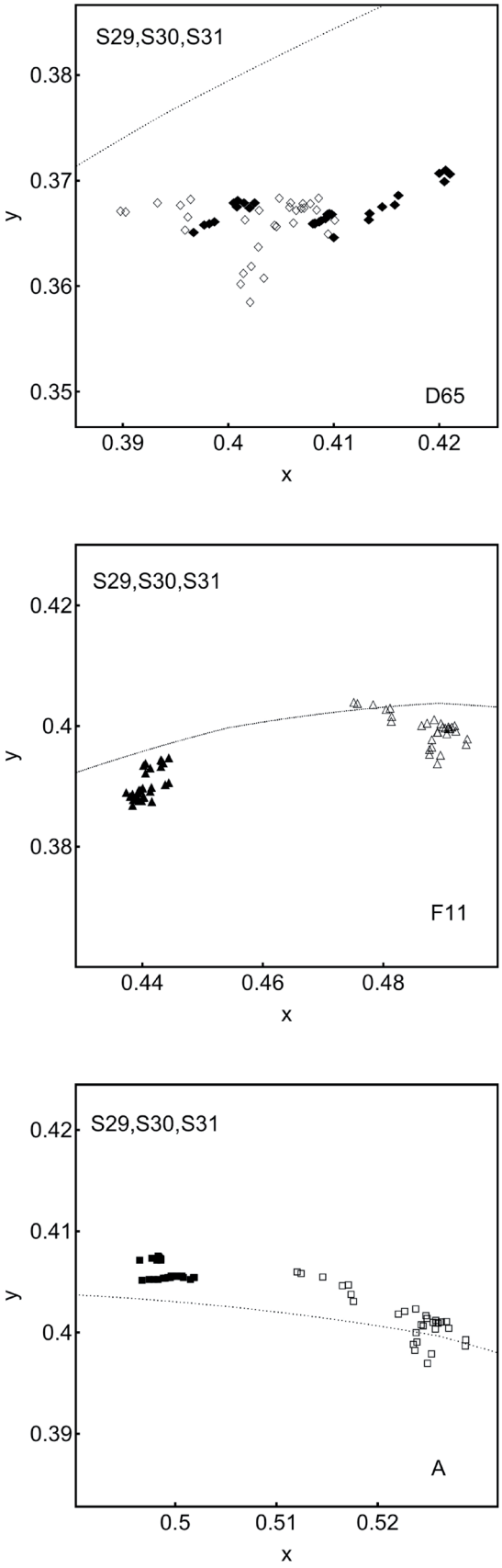

Fig. 12 Magnified xy chromaticity data for S29, S30 and S31 under the applied illuminations. Filled symbols: measured data; Open symbols: theoretical data

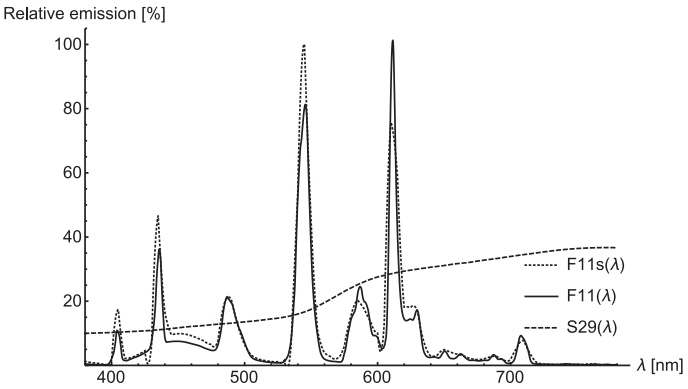

Fig. 13 Measured spectra of the applied sources (F11s theoretical, F11 measured spectra)

Tardos red limestone samples - S29, S30 and S31 - reflect more red lights thus the colorization effect of the applied illumination is more sensitive to differences in the higher spectral ranges. This difference explains the shift of the xy chromaticity data.

According to the colour difference calculations the white coloured stone slabs (S32, S55 and S56) the marble specimens, have different results than the other rock materials. The DeltaChroma and the DeltaE values of these white coloured specimens are higher than the other stones under all the three different lighting conditions. Only the DeltaChroma value of the white marble (S32) is smaller than that of the diorite (S861) under D65 illumination. The results of the three marble specimens, one white and two grey shows, that the little differences can be also perceived with this method. Mainly the grey ones have smaller DeltaChroma and DelteE values.

The red coloured specimens have lower DeltaChroma and DeltaE values - the lowest values related to the dark grey diorite. The red and grey limestones gave almost the same results. It is interesting that the values of the dark greenish grey Zuhánya limestone, is a little bit higher than the one of Tardos red limestone. Between the three Tardos red limestone specimens it is also possible to see slight differences – mainly under Illumiant A, and Illuminant F11 (Fig. 14, Fig. 15 and Fig. 16).

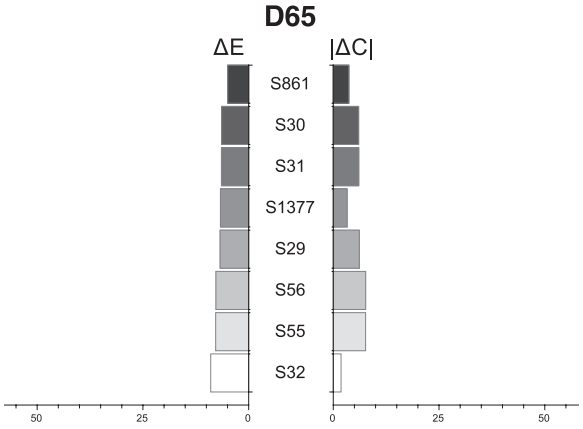

Fig. 14 ΔE and |ΔC| under Illuminant D65 compared to Illuminant E (S32-S861 represent no. of tested stone slabs – see Fig. 8)

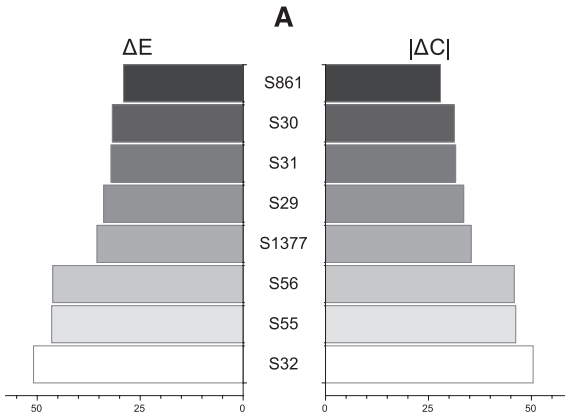

Fig. 15 ΔE and |ΔC| under Illuminant A compared to Illuminant E (S32-S861 represent no. of tested stone slabs – see Fig. 8)

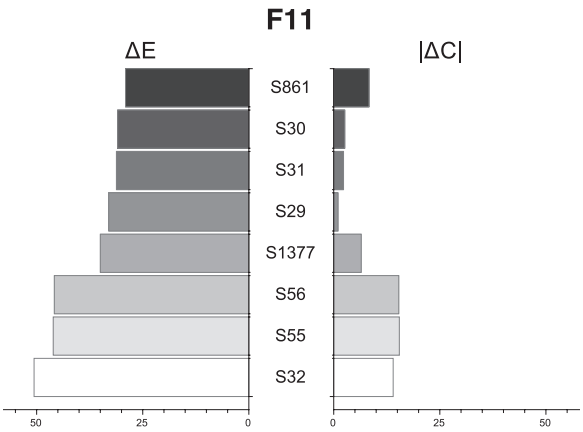

Fig. 16 ΔE and |ΔC| under Illuminant F11 compared to Illuminant E (S32-S861 represent no. of tested stone slabs – see Fig. 8)

5 Conclusions

Eight polished rock slabs representing five main lithologies were studied under different artificial lighting conditions to quantify colour differences and visual appearance of stone slabs.

According to the results of the calculations and the spectral measurements it is possible to divide the different stone materials by using colour spectra. In addition the applied method is capable to recognize changes in the colour of the stone slabs under different lighting conditions.

The five different dimension stones (two types of limestones, two types of marbles and a diorite) can be divided into two main colour classes: the light and the darker stones. The classification depicts significant differences between the spectral properties of very light marbles and the other darker stones. Within the group of darker stones marked differences were measured: Tardos red limestone and Siklós green limestone form one subgroup, while diorite represents another one. Consequently, this method can be used to classify not only the stones with high differences in colour, but it is also applicable to identify the slight differences in colour. With this colour measurement it was possible to recognize the slight difference between the three red Tardos limestone specimens.

The application of colour spectra measurements provides an additional tool for synchronizing the colour of the stone slabs with the applied lighting conditions. It is possible to use it as a design the colour effect of a stone slab with knowing the spectral properties of it.

Acknowledgement

The financial support of National Research, Development and Innovation (NKFI) Fund (K 116532) is appreciated.

References

[1] Zamora-Mestre, J.-L., Mesalles-Ruiz, J., Soriano-Gabarró, X. "Proposal for optical method of quality control of the surface of the slabs of natural stone for cladding facades." In: 37IAHS World Congress on Housing Science: "Design, Technology, Refurbishment and Management of Buildings", Santander, Spain, Oct. 26-29, 2010.

[2] Nagano, T., Nakashima, S. "Study of colors and degrees of weathering of granitic rocks by visible diffuse reflectance spectroscopy." *Geochemical Journal*. 23, pp. 75-83. 1989. DOI: 10.2343/geochemj.23.75

[3] CIE document 15:2004, Colorimetry, Technical Report, 2004.

[4] Hunt, R. W. G., Pointer, M. R. "*Measuring Colour*." John Wiley & Sons, Ltd. Published, 2011.

[5] Klein, G. A. "Industrial Color Physics." In: *Springer Series in Optical Sciences*. 154, Springer Science+Business Media, LLC 2010. DOI: 10.1007/978-1-4419-1197-1_2

[6] Choudhury, A. K. R. "*Principles of colour appearance and Measurement*." Woodhead Publishing Limited, Cambridge, 2014.

[7] MacAdam, D. L. "Color Measurement, Theme and Variations." Springer Verlag Berlin Heidelberg, 1985. DOI: 10.1007/978-3-540-38681-0

8] Ohta, N., Robertson, A. R. "Colorimetry Fundamentals and Applications." John Wiley & Sons Ltd, The Atrium, Southern Gate, Chichester,West Sussex, 2005.

[9] Schanda, J. (ed.) "*Colorimetry: understanding the CIE system*." John Wiley & Sons, Inc., Hoboken, New Jersey, 2007.

[10] Kertész, P. "Decay and conservation of Hungarian building stones." - In: Marinos, P. G., Koukis, G. C. (eds.) *The Engineering Geology of Ancient Works, Monuments and Historical Sites*. IEAG Conference Proceedings, Athens, Vol. II: 755-761. Balkema, Rotterdam, 1988.

[11] Török, Á. "Hungarian dimensional stones: an overview." *Zeitschrift der Deutschen Gesellschaft für Geowissenschaften*. 158(3), pp. 361-374, 2007.

[12] Pivko, D. "The provenance of stone tabernacle and altar table from the St. Emmeram's Cathedral (Nitra City)." *Acta Geologica Slovaca*. 1(2), pp. 119–124. 2009.

[13] Török, Á. "Petrophysical and sedimentological analyses of Siklós ornamental stones, S-Hungary." *Periodica Polytechnica Civil Engineering*. 43(2), pp. 187-205, 1999.

[14] Török, Á. "Formation of dolomite mottling in Middle Triassic ramp carbonates (Southern Hungary)." *Sedimentary Geology*. 131, pp. 131-145. 2000.

[15] Siegesmund, S., Török, Á. "Building Stones." In: Siegesmund, S., Snethlage, R. (eds.) *Stone in Architecture*. pp. 11-95. Springer, Berlin, 2011. DOI: 10.1007/978-3-642-14475-2_2

[16] Rosso, F., Pisello, A. L., Cotana, F., Ferrero, M. "Integrated Thermal-Energy Analysis of Innovative Translucent White Marble for Building Envelope Application." *Sustainability*. 6, pp. 5439-5462. 2014. DOI: 10.3390/su6085439

[17] Karaca, Z., Hacımustafaoğlu, R., Gökçe, M. V. "Grain properties, grain-boundary interactions and their effects on the characteristics of marbles used as building stones." *Construction and Building Materials*. 93, pp. 166–171. 2015. DOI: 10.1016/j.conbuildmat.2015.05.023

[18] Cardani, G., Meda, A. "Flexural strength and notch sensitivity in natural building stones: Carrara and Dionysos marble." *Construction and Building Materials*. 13(7), pp. 393–403. 1999. DOI: 10.1016/S0950-0618(99)00035-5

[19] Leiss, B., Weiss, T. "Fabric anisotropy and its influence on physical weathering of different types of Carrara marbles." *Journal of Structural Geology*. 22(11–12), pp. 1737–1745. 2000. DOI: 10.1016/S0191-8141(00)00080-8

[20] Borghi, A., Appolonia, L., Fiora, L., Zoja, A. "The grey marble of Porta Praetoria (Aosta, Italy): a minero-petrographic characterisation and provenance determination." *Periodico di Mineralogia*. 75, 2-3, pp. 59-74. 2006.